TITLE: Optical and Morphological Properties of Cu2FeSnS4 Chalcogenide Films

AUTHORS: Canan AYTUG AVA,Silan BATURAY

PAGES: 48-59

ORIGINAL PDF URL: https://dergipark.org.tr/tr/download/article-file/2451424

Yuzuncu Yil University

Journal of the Institute of Natural & Applied Sciences

Research Article

Optical and Morphological Properties of Cu₂FeSnS₄ Chalcogenide Films

Canan AYTUĞ AVA[*1,2], Şilan BATURAY[3]

[1] Dicle University, Institute of Natural Sciences, Department of Physics, 21280, Diyarbakir, Türkiye
[2] Dicle University, Science and Technology Application and Research Center, 21280, Diyarbakir, Türkiye
[3] Dicle University, Faculty of Science, Department of Physics, 21280, Diyarbakır, Türkiye
Canan AYTUĞ AVA, ORCID No: 0000-0003-4771-816X, Şilan BATURAY, ORCID No: 0000-0002-8122-6671
*Corresponding author e-mail: cananaytug@hotmail.com

Abstract: *P*-type Cu_2FeSnS_4 (CFTS) and Cu_2ZnSnS_4 (CZTS) quaternary chalcogenide films have been grown by the method of spin coating on glass substrates relate to 30 and 40 sccm sulfur flux. Physical properties of obtained samples were investigated by X-ray diffraction (XRD), scanning electron microscopy (SEM), atomic force microscopy (AFM) and ultraviolet visible spectroscopy (UV-Vis) to see the effect of deposition parameters on the thin film. The crystal parameters including crystal size, dislocation density and strain value of the samples were changed related to the deposition parameters. XRD results indicated an improvement of the crystalline quality of quaternary chalcogenide CFTS with a maximum crystal size of about 50 nm for (112) peak orientation. SEM images illustrated that the particle size was changed with an increase in the flux of sulfur, which was confirmed with both XRD and AFM images. It was seen that the absorption and energy band gap value of the samples changed the effect of sulfur flux and CZTS film for 40 sccm exhibited more strong absorption all samples in the UV-Vis region. The band gap values of the samples were calculated 1.51, 1.53, 1.82 and 1.91 eV for CZTS (30 sccm), CZTS (40 sccm), CFTS (30 sccm) and CFTS (40 sccm) films annealed H_2S gas, respectively.

Cu₂FeSnS₄ Kalkojenit Filmlerin Optik ve Morfolojik Özellikleri

Öz: *P*-tipi Cu_2FeSnS_4 (CFTS) ve Cu_2ZnSnS_4 (CZTS) kuaterner kalkojenit filmler, 30 ve 40 sccm kükürt akışıyla ilgili cam alt-tabakalar üzerinde döndürmeli kaplama yöntemiyle büyütülmüştür. Elde edilen numunelerin fiziksel özellikleri, X-ışını kırınımı (XRD) ölçüm sistemi, taramalı elektron mikroskobu (SEM), atomik kuvvet mikroskobu (AFM) ve ultraviyole görünür (Uv-vis) spektrofotometre ölçüm sistemi ile araştırılarak ince filmlerin biriktirme parametrelerinin etkisi incelenmiştir. Numunelerin kristal boyutu, dislokasyon yoğunluğu ve gerinim değeri gibi kristal parametreleri biriktirme parametrelerine bağlı olarak değişmektedir. XRD sonuçları, (112) pik yönelimi için yaklaşık 50 nm maksimum kristal boyutu ile kuaterner kalkojenit CFTS'nin kristal kalitesinde bir gelişmeyi gösterir. SEM görüntüleri hem XRD hem de AFM görüntüleri ile teyit edilen, kükürt akışındaki artışla parçacık boyutunun değiştiğini göstermektedir. Örneklerin absorpsiyon ve enerji bant aralığı değerinin kükürt akışının etkisini değiştirdiği ve 40 sccm için CZTS filmi, Uv-vis bölgesindeki tüm numunelerden daha güçlü absorpsiyon göstermiştir. Örneklerin bant aralığı değerleri, H_2S gazında tavlanan CZTS (30 sccm), CZTS (40 sccm), CFTS (30 sccm) ve CFTS (40 sccm) filmler için sırasıyla 1.51, 1.53, 1.82 ve 1.91 eV olarak hesaplanmıştır.

1. Introduction

Cu$_2$XSnS$_4$ (X= Fe, Zn, Ni, Mn, Co) (Ansari et al., 2019; Elsaeedy, 2019; Krishnaiah et al., 2019; Rudisch et al., 2019; Zhou et al., 2019) films which are known as quaternary chalcogenides have been attracted extra consideration due to their physical and chemical properties including semiconducting and optical properties for the application of photovoltaic. These chalcogenides show conductivity of *p*-type and are used as absorbers in the application of solar cell. These chalcogenides also possess an optical band gap in the around 1.0–1.5 eV (Rudisch et al., 2019), a good absorption value (10^4 cm^{-1}) coefficient (Guan et al., 2014) and a high electrical mobility value about 11.44 cm^2 V^{-1} s^{-1} (Prabhakar et al., 2014). Different types of absorber layers for solar cells, with good absorption coefficient value and suitable optical energy band gaps resembles to CIGS (Cu(InGa)Se$_2$) films have been recently attracted considerable interst in some experimental applications like optoelectronic and photovoltaic and solar cell due to their good power conversion efficiency (Jackson et al., 2011; Friedlmeier et al., 2015). However, the high cost and non abundance of gallium (Ga) and indium (In) elements limit the production of Cu(InGa)Se$_2$ films as absorber layer in solar cells. Monsefi & Kuo (2014) have recently studied electrical properties of Mg:CIGSe$_2$ film using method of liquid phase sintering. They indicated a charge carrier concentration of 2.86×10^{16} cm^{-3} and mobility value of 4.23 cm^{2}V^{-1}S^{-1} was gained for 10% Mg:CIGS compared to 3.25×10^{16} cm^{-3} carrier concentration and 1.16 cm^{2}V^{-1}s^{-1} mobility value for the 0%Mg:CZTS. Among most promising material for photovoltaic films that may replace CIGS is the quaternary chalcogenide CFTS (Cu$_2$FeSnS$_4$) and CZTS (Cu$_2$ZnSnS$_4$) which has the main advantages with low cost and its non toxic formation process. In recent years, several studies have been carried out on the structural, optical and electrical properties of CFTS and CZTS thin films (Meng et al., 2015; Miao et al., 2017; Wang et al., 2017). CFTS films show stannite tetragonal type, which is derived from a type of zinc blende. In stannite tetragonal structure, anion sulfur is encircled by two copper, one ıron and one tin and every cation is tetrahedrally organized by sulfur. It has been theoretically demonstrated that the presence of stannite tetragonal type coordinated semi-conductor in which each anion sulphur is encircled by four cations and each cation is tetrahedrally organized by four sulfur anion is a critical feature for the exhibition of excellent photovoltaic properties of chalcogenide absorber materials (Domain et al., 2003). Additionally, it possess a suitable energy band gap value of between 1.2 and 1.5 eV (Mokurala et al., 2014; Wang et al., 2014; Meng et al., 2015) for absorber material in application of photovoltaic and a good value of absorption up to 10^5 cm^{-1} (Guan et al., 2014). Therefore, in this work, we have systematically varied sulphur flow and doping effect to obtain a better Cu based multinary chalcogenide absorber material by using a spin coating for better results.

Shape controlled topologies, doping elements and thin film deposition parameters have a significant role in the thin film's physical properties in the nanoscale region. Also, a lots metal can be employed as doping elements to improve the quality of crystalline thin films' properties with excellent physical and chemical properties of nanostructured thin films. Abundant and environment-friendly quaternary CFTS films have been grown by different fabrication methods such as the spray pyrolysis method (Nefzi et al., 2020b), electrochemical deposition technique (Miao et al., 2017), chemical method (Nefzi et al., 2018), RF-magnetron sputtering (Meng et al., 2015a), chemical spray pyrolysis (Khadka & Kim, 2015) and spin coating (Dong et al., 2018). To our knowledge, there is limited information on the effect of sulfur on the physical properties of CFTS films fabrication using different techniques (Meng et al., 2015b; Meng et al., 2017). There is also no work in the literature on the effect of sulfur flux on physical properties of CFTS film using the spin coating technique. However, these deposition systems have some disadvantages, such as costly vacuum conditions, expensive precursors, and difficulties in substrate temperature. Compared with these deposition techniques, spin-coating is a very efficient method in transition metal oxide due to its adjustable fabrication rate, its advantages of low cost and flexible substrate temperature.

Sulfur flux has a large impact on the crystal parameters and optical properties of CZTS and CFTS film (Mokurala et al., 2014). The main gain of our work is to investigate the effect of varying sulphur flux rate and ion effect (Zn^{2+} Fe^{3+}) in order to improve the crystal and optical properties of CZTS and CFTS thin films. Thus, to get more light on the understanding of the effect of sulfur flux on the physical properties of CFTS film, more experimental studies are necessary. For this reason, we are focused on the modified the physical properties of CZTS and CFTS samples related to the sulfur flux rate. We have successfully fabricated CZTS and CFTS thin films related to 30 and 40 sccm H$_2$S:Ar(1:9)

rate by spin coating on glass substrates using ethanol solvent and glacial acetic acid (GAA). Physical properties including crystal parameter, morphological properties, absorbance and energy band gap were studied by X-ray diffraction (XRD) system, scanning electron microscopy (SEM), atomic force microscopy (AFM) and ultraviolet visible spectroscopy (UV-Vis) system to get more knowledge about CZTS and CFTS quaternary semiconductor needing further widespread works on physical parameters of the film.

2. Material and Methods

Quaternary chalcogenide CFTS and CZTS films at various annealing conditions were deposited on well-cleaned glass substrates by the spin coating method at a 240 °C substrate temperature. The films under two different annealing conditions were deposited by using 0.2 M cupric chloride ($CuCl_2$), 0.1 M Ferrous (II) chloride dehydrate ($FeCl_2$), 0.04 M Zinc chloride ($ZnCl_2$), and 0.1 M tin (II) chloride dihydrate ($Cl_2Sn.2H_2O$) as copper, iron, zinc and tin source, respectively. The chemical with a 2:1:1 stoichiometric ratio was separately prepared in a mixture of 50 ml ethanol, 5 ml GAA and a small amount of diethanolamine and mixed for 2 h on a magnetic stirrer at room temperature. During the preparation of homogenous white solutions to gain CFTS thin film, $FeCl_2$ solution was added to the cupric chloride solution, and finally, the corresponding amount of tin(II) chloride dihydrate solution was added to the iron/cupric chloride solution. Also, during the preparation of homogenous white solutions to gain CZTS thin film, $ZnCl_2$ solution was added to the cupric chloride solution, and finally, the corresponding amount of tin(II) chloride dihydrate solution was added to the zinc/cupric chloride solution. To obtain clear and homogenous films and remove any residual waste, the glass substrates and glass bottles were cleaned by boiling in adequate quantities of H_2O (distilled water), NH_3 (ammonia), and H_2O_2 (hydrogen peroxide) mixtures at 105 °C and then in adequate quantities of H_2O, H_2O_2, and HCl (hydrochloric acid) mixtures at the same condition before fabrication process. Then each, substrates and glass bottles were cleaned in deionized water for 3 min and dried in N_2 atmosphere. After obtaining the final solutions and cleaning the substrates, the CFTS and CZTS films with 2:1:1 stoichiometric ratios were seperately spin coated on substrates at a rate of 5000 rpm for 55 s in air condition as reference. The final solutions were dropped onto the substrate by layer and layer, and obtained samples were preheated to 240 °C for 10 min in air. Having obtained 10 layers of CFTS and CZTS samples, these samples were gradually annealed in a quartz furnace at 30 and 40 sccm H_2S:Ar flows for 90 minutes at 550 °C, respectively. The sample names were CFTS(I) and CFTS(II) for 30 sccm and 40 sccm sulfur flux and CZTS(I) and CZTS(II) for 30 sccm and 40 sccm sulfur flux, respectively.

Structural analysis, including crystal parameters, was performed using a Rigaku ultima III diffractometer system between 20° and 60°. Topologies and composition of the films were analyzed by SEM and AFM. Optical properties including absorbance and energy gap were studied by UV-Vis spectrophotometer in the wavelength range of 1100-300 nm at room temperature under air atmosphere as reference.

3. Results and Discussion

3.1. Structural properties

The crystal parameters and quality of the grown samples were determined from the results of the XRD data. Figure 1 displays the XRD spectrum of the *p*-type quaternary CZTS and CFTS samples annealed at 550 °C. The CZTS thin films annealed under 30 and 40 sccm sulphur flows which exhibited about $2\theta \approx 28.52°, 47.40°$, and $56.23°$ could be indexed to (112), (220) and (312) crystal planes of kesterite structure. The intensity of the peak around 28.52° is stronger than other peaks and indicates preferential orientation. When the XRD patterns of the thin films with Fe substitution was analyzed, it was seen that the XRD patterns of the samples which exhibited about $2\theta \approx 28.80°$ could be indexed to the (112), 47.60° could be indexed to the (204) plane and the weak diffraction peaks at about 33.27° could be indexed to the (200) plane of the stannite CFTS thin film. It showed that Fe atoms were joined with CTS in the unit cell volume annealed sulfur flux. In addition, the XRD results of CFTS samples exhibited sharp peaks that correspond to the dominant (112) orientation. A change in the

FWHM and the intensity of all thin film peaks by XRD data can be seen in Figure 1. The intensity of the main peak was almost unchanged as the intensity of (204) plane decreased. The (112) and (204) planes of the samples showed a shift in peak position. (Wang et al., 2017) indicated that CFTS films obtained from the blade-coating process were crystallized in a similar structure.
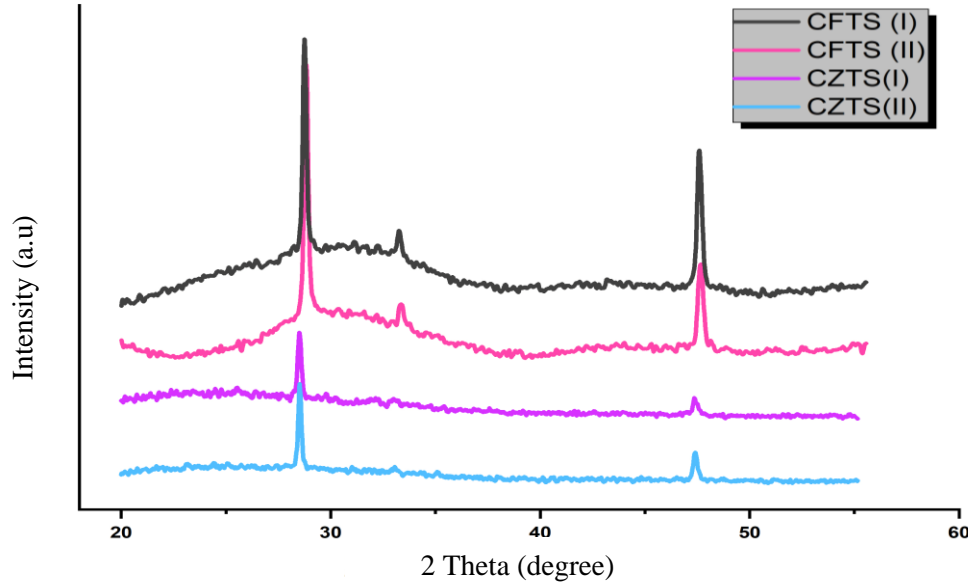

Figure 1. XRD patterns of CZTS and CFTS film annealed at H_2S:Ar flow.

The theoretically calculated interplanar spacing (d), the crystal size (D), the dislocation density (δ) and the values of strain (ε) for all peaks for the obtained samples are given in Table 1. As understood from this table, the position of main peak (112) planes shifted from 28.75° to 28.83° and (002) planes shifted from 47.59° to 47.66° for the CFTS samples under increasing sulfur flux while this shift was attributed to the increase of H_2S:Ar flow rate on the crystal structure of the obtained samples and also Fe^{3+} and Zn^{2+} substitution influence on the crystal parameters of the film. The difference in the ionic radius of Zn and Fe substitution caused disorder in the lattice parameters, resulting in changing of peak orientation towards the higher diffraction angle. Scherer's equation which is used to determine the D value of obtained samples from the XRD data is described as (Cullity, 1956):

$$D = \frac{k\lambda}{\beta cos\theta} \tag{1}$$

where λ is the wavelength (λ = 1.540056 Å), β is the FWHM value of the peaks, θ is the Bragg's angle in degree, and k is the constant which shows shape factor (k = 0.89). As seen from the table 1, the value of crystal size corresponding to (112) planes for CZTS(II) film was higher than the CZTS(I) film. WhenFe substitution was added, the crystal size value was rapidly increase. The D corresponding main planes for the CFTS(I) (50.43 nm) were higher than the all samples, which can be seen from table. The maximum D value of the samples was found to be 50.43 nm, corresponding to the main peak for CFTS(I) thin film. The largest D value of the main peak showed that precursors might be transformed into samples with good crystalline quality. The calculated results displayed the D value of the samples was changed with H_2S:Ar flows. This calculated crystal size value was higher than in earlier studies (Adelifard, 2016; Nilange et al., 2019). Nanocrystals in the samples must form a bigger crystal size in order to gain high solar cell effectiveness (Tanaka et al., 2006).

Table 1. XRD samples of CFTS thin films annealed in sulphur flux at 550°

Sample	2θ (Derece)	D (nm)	d (calculated) (Å)	δ (10^{14} m^2)	ε (X10^{-3})	hkl
CZTS (I)	28.51	32.15	3.13	9.67	4.4	112
CZTS (II)	28.52	33.53	3.13	8.90	4.2	112
CFTS (I)	28.75	50.4	3.11	3.93	2.9	112
	47.59	35.9	1.91	7.77	2.5	204
CFTS (II)	28.83	43.7	3.11	5.23	3.3	112
	47.66	31.6	1.91	10	2.9	204

d, δ and ε value of the CFTS samples were calculated by the equation (2), (3) and (4), respectively (Shaikh et al., 2011; Tiong et al., 2014):

$$2\mathrm{d}sin\theta = n\lambda$$

(2)

$$\delta = \frac{1}{D^2}$$

(3)

$$\varepsilon = \frac{\beta cos\theta}{4}$$

(4)

where n is a constant which gives the order of diffraction, strain (ε) and dislocation density (δ) value of all films which is one of the significant factors negatively changing the crystal structure. We can see from Table 1 that the calculated d value of the both CFTS and CZTS thin films annealed under 30 sccm sulphur flow was close to the both CFTS and CZTS thin film annealed under 40 sccm sulphur flows. The calculated d value of the thin films complies with the standard values. In our study, the value d was decreased from 3.13 to 3.11 Å after substituting Fe atom. This result can be owing to the different atomic radii of Fe atom compared to Zn atom.

As seen from table, the calculated dislocation density values of CZTS(I) and CZTS(II) for main peak were 9.67 and 8.90 $\times 10^{14}$ m^{-2}, respectively. The calculated δ values of the main peak for CFTS(I) were changed between 3.93 $\times 10^{14}$ m^{-2} and 7.77 $x\ 10^{14}$ m^{-2}. The minimum value of δ was found to be 3.93 $\times 10^{14}$ m^{-2} for CFTS(I) film, which displayed the better crystallinity of the film because δ was a measurement of the quantity of defect. Nefzi et al. (2020a) indicated that dislocation density was found to be between 25 $\times 10^{13}$ m^{-2} to a minimum value of 4.93 $\times 10^{13}$ m^{-2}. When these values were examined for the main peak, both δ and ε values were changed depending on sulfur flux. The change in the calculated δ values indicated the presence of strain in the films. The variation in the strain was related to the lattice defects being dependent on the deposition parameter. It can be seen from these results that the reason for the change in crystal size is the change in strain. As the sulfur flux increased, the increase in strain value in thin films belonging to the main peak caused an increase in lattice defects and affected the quality of the obtained film.

3.2. Morphological properties

The surface morphologies of the obtained samples are very important for analyzing the surface properties of thin films. Figure 2 shows SEM images of samples with different sulfur flux grown using the spin coating method. It is seen that the films have less uniform surface, although there are very few defects such as cracks and voids in Figure 2. The samples obtained appear to be relatively uniformly dispersed with little agglomeration to the substrate due to more interactions between the thin films and sulphur flow. As seen in Figure 2. there is a difference in CFTS and CZTS morphology as they tend to be like spherical nanostructured films with more uniformly distribution and small agglomeration. It can be seen from SEM images that the surfaces of the CFTS(I) thin films is more homogeneous than all thin film.
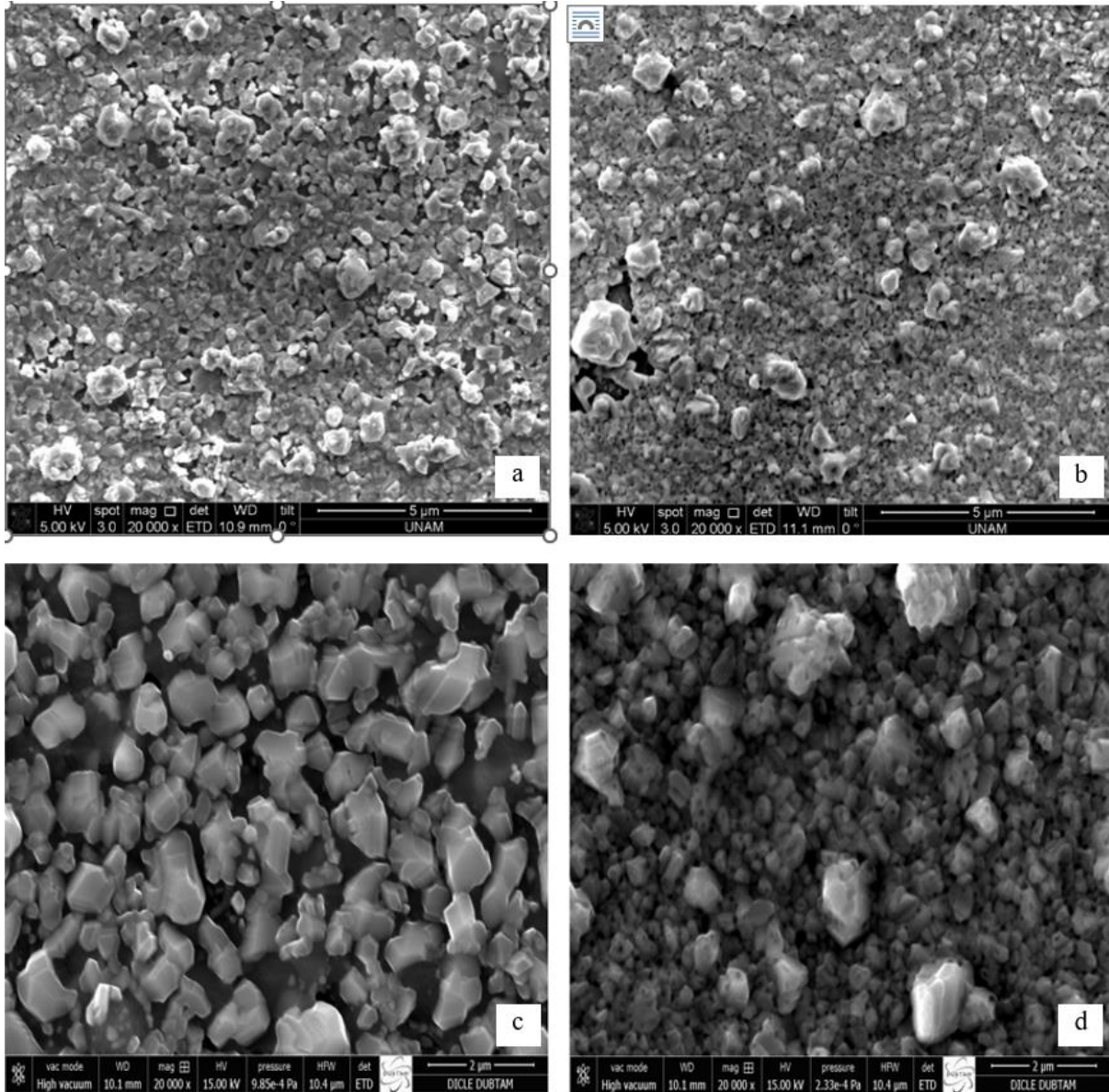
Figure 2. SEM images of a) CZTS(I), b) CZTS (II), c) CFTS(I), d) CFTS(II) samples.

Figure 3(a-b) displays the topology of both CFTS and CZTS samples annealed H$_2$S:Ar ambient by AFM images. The CFTS(I) sample displays bigger lumps than the CFTS(II) sample while the CZTS(II) sample displays bigger lumps than the CZTS(I) sample. The figures indicate thin films with the structure of grain particles. The AFM tip photographs the seeming of the samples and does not go deep to describe the size of the particle. Nevertheless, if some spaces on the samples have gaps, the tip gives that as the valley and the superficial of the sample appear both bumpy and cloggy, just what occurred here for the obtained samples. The obtained sample outcome is less uniform and grain particles have been placed in an inhomogeneous manner. The obtained results are consistent with previous studies (Madhusudanan et al., 2019).
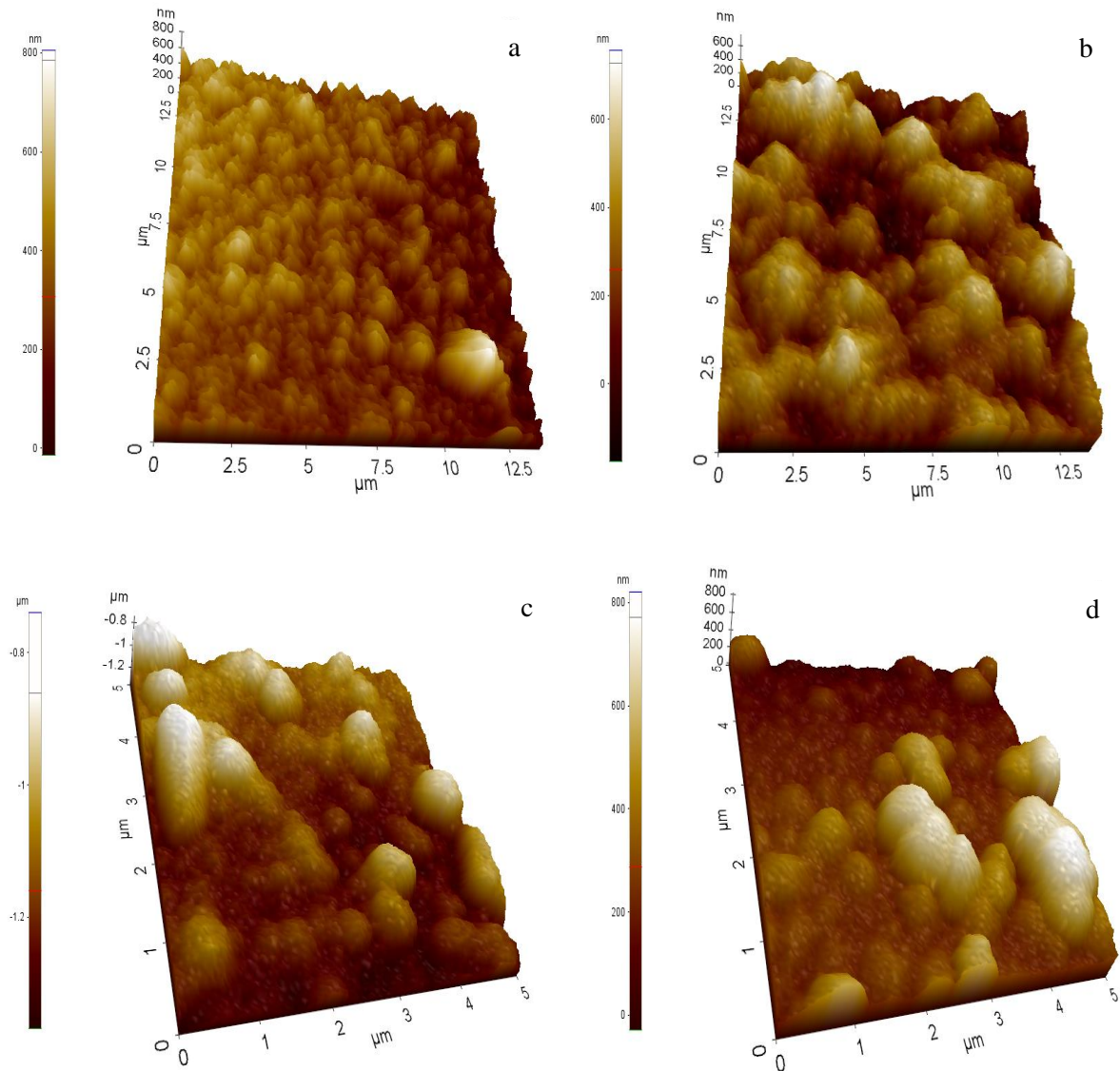
Figure 3. AFM images of a) CZTS(I), b) CZTS (II), c) CFTS(I), d) CFTS(II) samples.

3.3. Optical properties

The absorbance and transmittance of used nanostructured materials can be effected by many variables like the deposition technique, surface topology, and some deposition conditions (temperature, film thickness, annealed time), related to their interaction with the ambient. Furthermore, the absorbance-wavelength of CZTS and CFTS films were analyzed using UV–Vis data gained between 1100 and 300 nm wavelength. The analysis of the value of absorption coefficient for any nanostructured thin film gives extra knowledge concerning the levels of electrons in the high-energy range of the absorption spectra, while the low-energy range of the absorption spectrum relate to the atoms' vibration (Urbach, 1953; El-Hagary et al., 2012). It can be seen from Figure 4, CZTS(II) film exhibit more strong absorption than all other thin film in the all-region. The increase in sulfur flux rate and exchange in Zn^{2+}and Fe^{3+} may also induce a change in absorbance values. From these absorption spectra, we noted That absorption of CFTS(I) film has the minimum absorption value while CZTS(II) has the maximum. As seen from the Figure 4, all samples have high absorption till the region of infrared. The decreasing absorption tendency in the Fe incorporated films visible region is lower than the pure CZTS thin film. It is seen from these results that the CZTS and CFTS samples have sensitive to absorption in the UV-vis range. The change in the absorption value of the samples indicates that obtained thin films can be

applied in various optical applications including optical windows and suitable materials for UV filter production.
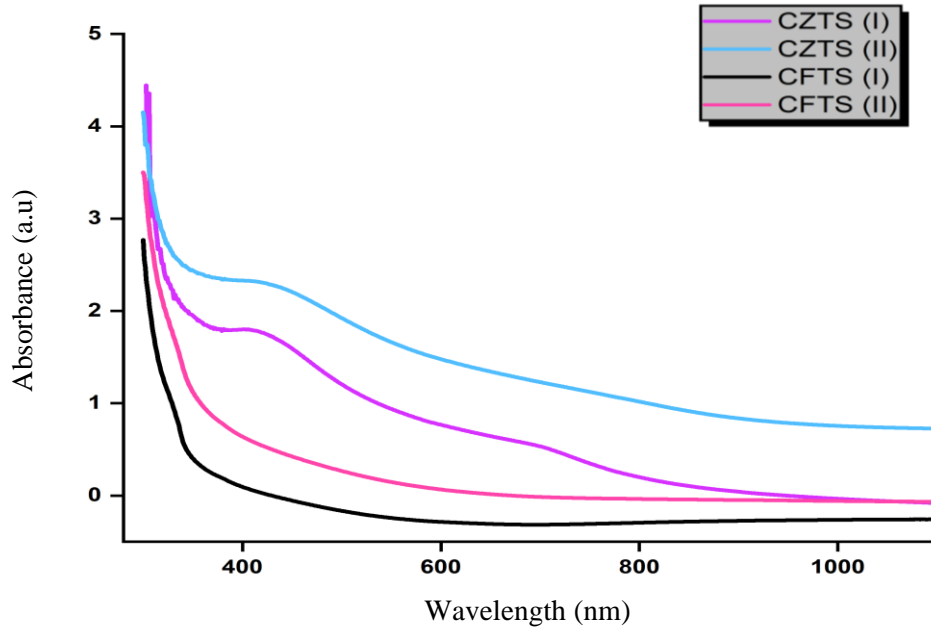

Figure 4. Absorption spectra of CFTS thin films.

The band-gap (E_g) of the CZTS and CFTS samples was calculated using relation of Tauc (2012):

$$\alpha h v = A(hv - Eg)^m \tag{5}$$

where A is the material's energy independent constant, m is constant that based on the transition nature, $m = 1/2, 2, 3/2$, or 3 for direct, nondirect allowed transition, forbidden direct or forbidden nondirect transitions, respectively. α is a constant that gives the coefficient of absorption in cm^{-1} and λ is the wavelength. plot of $(\alpha h v)^2$ versus photon energy (hv) for the obtained samples with sulphur flux at 550 °C is given in Figure 5. As seen Figure 5, the linear nature of all energy band gap graphs indicates that CZTS and CFTS semiconductors have the direct band gap.

Figure 5 indicates the E_g value of CZTS and CFTS films, and the E_g value is calculated to be 1.51, 1.53, 1.82 and 1.91 eV for CZTS(I), CZTS(II), CFTS(I) and CFTS(II) films, respectively. The obtained energy band gap value of CZTS thin film was given previous study (Ava et al., 2021). The change in band gap value might be owing to the difference in the crystallinity nature of the film, which is seen from XRD data. The increasing of energy band gap values was owing to the effect of the change of crystalline quality and ionic radius of Zn^{2+}(0.74Å) and Fe^{3+}(0.55Å) ions in obtained films. The obtained energy band values were different from the previous studies of 1.37, 1.42 and 1.71 eV (Khadka & Kim, 2015; Hannachi et al., 2017; Vanalakar et al., 2018) which attributed to the different annealed condition, deposition method and element composition. We noted that the band gap value of the CZTS and CFTS samples is in good agreement with those given previously (Nefzi, 2020b).The increase of E_g values was due to the effect of the change of crystalline quality in obtained CFTS films. In this study, we experimentally showed that the cationic substitution of Zn by Fe could change the physical properties including absorbance and energy band gap of CZTS material.
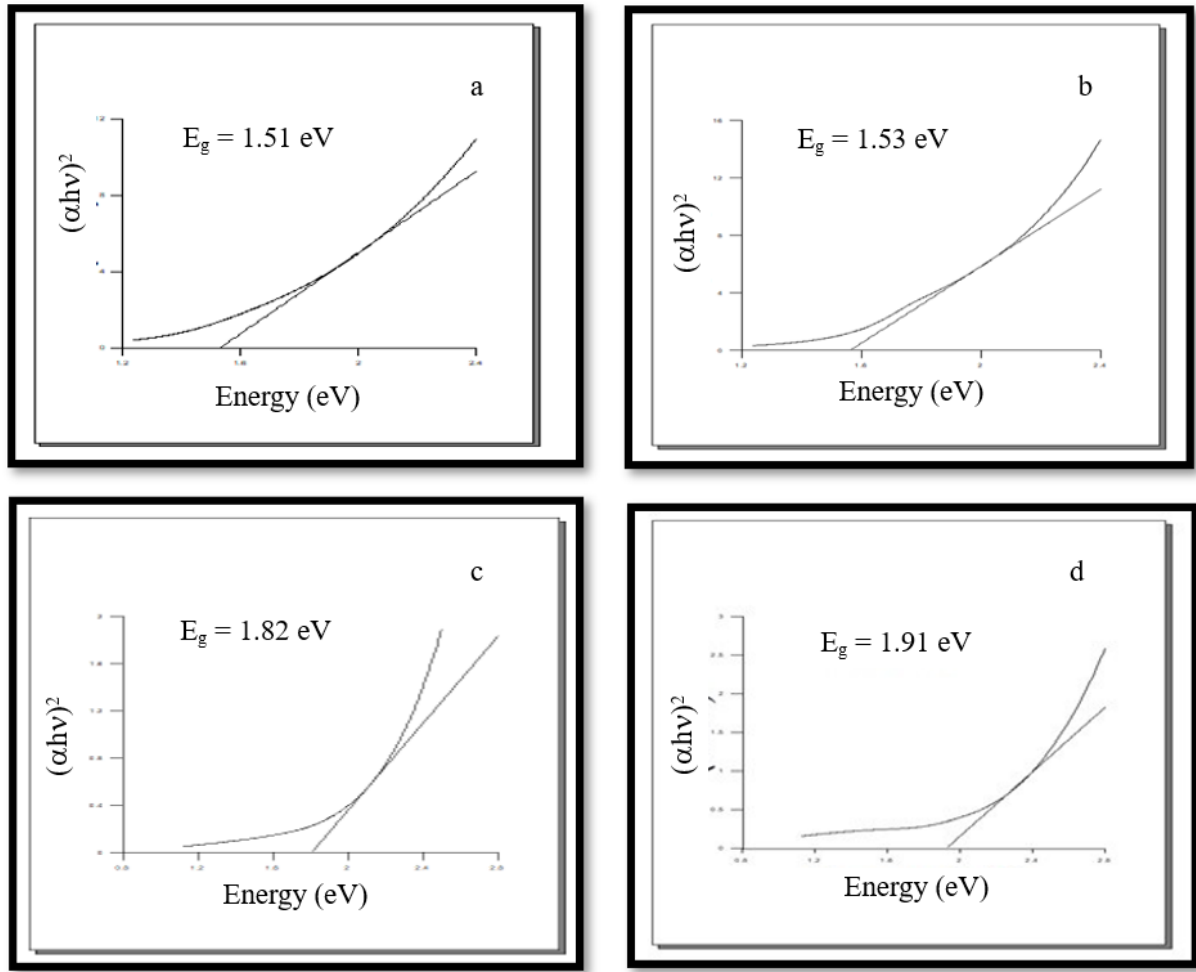
Figure 5: Energy band gap of a) CZTS(I), b) CZTS(II), c) CFTS(I) and d) CFTS(II) film.

4. Conclusion

In summary, in this study, CFTS and CZTS thin films with different sulfur flows were obtained annealed at 550 °C using the spin coating technique. The effect of sulfurization on the structural, morphological and optical properties of the film were investigated XRD, SEM, AFM and UV-Vis measurement system. The maximum D value of the samples was found to be 50.43 nm, corresponding to the main peak for CFTS(I) thin film. The calculated δ value of the main peak for CFTS(I) film was changed between $3.93 \, x \, 10^{14}$ m^{-2} and $7.77 \, x \, 10^{14}$ m^{-2}. The minimum value of calculated δ was found as $3.93 \, x \, 10^{14}$ m^{-2} for CFTS(I), which displayed the better crystallinity of the film. When the surface properties of the films were examined, it was seen that spherical-like nanostructures were formed and the number of these nanoparticles increased depending on the sulfur flux. It was observed that CZTS(II) film exhibit more strong absorption than all other thin film in the all-region. The films had strong absorption in the UV region and a strong affinity for UV light. The energy band gap values of the obtained samples were calculated as 1.51, 1.53, 1.82 and 1.91 eV for CZTS(I), CZTS(II), CFTS(I) and CFTS(II) films, respectively and it was seen that the sulfur flux affected the energy band gap and absorbance value.

Acknowledgements

References

Adelifard, M. (2016). Preparation and characterization of Cu_2FeSnS_4 quaternary semiconductor thin films via the spray pyrolysis technique for photovoltaic applications. *Journal of Analytical and Applied Pyrolysis*, 122, 209-215. doi:10.1016/j.jaap.2016.09.022

Ansari, M. Z., Singh, S., & Khare, N. (2019). Visible light active CZTS sensitized CdS/TiO₂ tandem photoanode for highly efficient photoelectrochemical hydrogen generation. *Solar Energy*, 181, 37-42. doi:10.1016/j.solener.2019.01.067

Ava, C. A., Ocak, Y. S., Asubay, S., & Celik, O. (2021). The influence of Ge substitution and H₂S annealing on Cu_2ZnSnS_4 thin films. *Optical Materials*, 121, 111565. doi:10.1016/j.optmat.2021.111565

Cullity, B. D. (1956). *Elements of X-ray diffraction*: Boston, USA: Addison-Wesley. ISBN-0201012308.

Domain, C., Laribi, S., Taunier, S., & Guillemoles, J. F. (2003). Ab initio calculation of intrinsic point defects in CuInSe2. *Journal of Physics and Chemistry of Solids*, 64(9-10), 1657-1663. doi:10.1016/S0022-3697(03)00208-7

Dong, C., Ashebir, G. Y., Qi, J., Chen, J., Wan, Z., Chen, W., & Wang, M. (2018). Solution-processed Cu_2FeSnS_4 thin films for photovoltaic application. *Materials Letters*, 214, 287-289. doi:10.1016/j.matlet.2017.12.032

El-Hagary, M., Emam-Ismail, M., Shaaban, E., & El-Taher, A. (2012). Effect of γ-irradiation exposure on optical properties of chalcogenide glasses Se70S30− xSbx thin films. *Radiation Physics and Chemistry*, 81(10), 1572-1577. doi:10.1016/j.radphyschem.2012.05.012

Elsaeedy, H. I. (2019). Growth, structure, optical and optoelectrical characterizations of the Cu2NiSnS4 thin films synthesized by spray pyrolysis technique. *Journal of Materials Science: Materials in Electronics*, 30(13), 12545-12554. doi:10.1007/s10854-019-01615-3

Friedlmeier, T. M., Jackson, P., Bauer, A., Hariskos, D., Kiowski, O., Wuerz, R., & Powalla, M. (2015). Improved photocurrent in Cu(In, Ga)Se₂ solar cells: from 20.8% to 21.7% efficiency with CdS buffer and 21.0% Cd-free. *IEEE Journal of Photovoltaics*, 5(5), 1487-1491. doi:10.1109/PVSC.2015.7356152

Guan, H., Shen, H., Jiao, B., & Wang, X. (2014). Structural and optical properties of Cu_2FeSnS_4 thin film synthesized via a simple chemical method. *Materials Science in Semiconductor Processing*, 25, 159-162. doi:10.1016/j.mssp.2013.10.021

Hannachi, A., Oueslati, H., Khemiri, N., & Kanzari, M. (2017). Effects of sulfurization on the optical properties of $Cu_2ZnxFe1-xSnS_4$ thin films. *Optical Materials*, 72, 702-709. doi:10.1016/j.optmat.2017.07.031

Jackson, P., Hariskos, D., Lotter, E., Paetel, S., Wuerz, R., Menner, R., Wischmann, W., & Powalla Prog, M., (2011). New world record efficiency for Cu(In,Ga)Se2 thin-film solar cells beyond 20%. *Photovoltaics*, 19, 894-897. doi:10.1002/pip.1078

Khadka, D. B., & Kim, J. (2015). Structural, optical and electrical properties of Cu2FeSnX4 (X= S, Se) thin films prepared by chemical spray pyrolysis. *Journal of Alloys and Compounds*, 638, 103-108. doi:10.1016/j.jallcom.2015.03.053

Krishnaiah, M., Mishra, R. K., Seo, S. G., Jin, S. H., & Park, J. T. (2019). Highly crystalline, large grain Cu2CoSnS4 films with reproducible stoichiometry via direct solution spin coating for optoelectronic device application. *Ceramics International*, 45(9), 12399-12405. doi:10.1016/j.ceramint.2019.03.167

Madhusudanan, S. P., Mohanta, K., & Batabyal, S. K. (2019). Electrical bistability and memory switching phenomenon in Cu2FeSnS4 thin films: role of pn junction. *Journal of Solid State Electrochemistry*, 23(5), 1307-1314. doi:10.1007/s10008-019-04213-9

Meng, X., Deng, H., He, J., Sun, L., Yang, P., & Chu, J. (2015a). Synthesis, structure, optics and electrical properties of Cu2FeSnS4 thin film by sputtering metallic precursor combined with rapid thermal annealing sulfurization process. *Materials Letters*, 151, 61-63. doi:10.1016/j.matlet.2015.03.046

Meng, X., Deng, H., Sun, L., Yang, P., & Chu, J. (2015b). Sulfurization temperature dependence of the structural transition in Cu2FeSnS4-based thin films. *Materials Letters*, 161, 427-430. doi:10.1016/j.matlet.2015.09.013

Meng, X., Deng, H., Zhang, Q., Sun, L., Yang, P., & Chu, J. (2017). Investigate the growth mechanism of Cu2FeSnS4 thin films by sulfurization of metallic precursor. *Materials Letters*, 186, 138-141. doi:10.1016/j.matlet.2016.10.002

Miao, X., Chen, R., & Cheng, W. (2017). Synthesis and characterization of Cu2FeSnS4 thin films prepared by electrochemical deposition. *Materials Letters*, 193, 183-186. doi:10.1016/j.matlet.2017.01.099

Mokurala, K., Bhargava, P., & Mallick, S. (2014). Single step synthesis of chalcogenide nanoparticles Cu_2ZnSnS_4, Cu_2FeSnS_4 by thermal decomposition of metal precursors. *Materials Chemistry and Physics*, 147(3), 371-374. doi:10.1016/j.matchemphys.2014.06.049

Monsefi, M., & Kuo, D. H. (2014). Influence of Mg doping on electrical properties of Cu(In, Ga)Se₂ bulk materials. *Journal of Alloys and Compounds*, 582, 547-551. doi:10.1016/j.jallcom.2013.08.101

Nefzi, C., Souli, M., Cuminal, Y., & Kamoun-Turki, N. (2018). Effect of sulfur concentration on structural, optical and electrical properties of Cu_2FeSnS_4 thin films for solar cells and photocatalysis applications. *Superlattices and Microstructures*, 124, 17-29. doi:10.1016/j.spmi.2018.09.033

Nefzi, C., Souli, M., Cuminal, Y., & Kamoun-Turki, N. (2020a). Effect of sprayed volume on physical properties of Cu_2FeSnS_4 thin films and an efficient p-type Cu2FeSnS4/n-type F-doped SnO2 heterojunction. *Journal of Physics and Chemistry of Solids*, 144, 109497. doi:10.1016/j.jpcs.2020.109497

Nefzi, C., Souli, M., Jeyadevan, B., & Kamoun-Turki, N. (2020b). Effect of substrate temperature on physical properties of Cu_2FeSnS_4 thin films for photocatalysis applications. *Materials Science and Engineering: B*, 254, 114509. doi:10.1016/j.mseb.2020.114509

Nilange, S. G., Patil, N. M., & Yadav, A. A. (2019). Growth and characterization of spray deposited quaternary Cu2FeSnS4 semiconductor thin films. *Physica B: Condensed Matter*, 560, 103-110. doi:10.1016/j.physb.2019.02.008

Prabhakar, R. R., Huu Loc, N., Kumar, M. H., Boix, P. P., Juan, S., John, R. A., Wong, L. H. (2014). Facile water-based spray pyrolysis of earth-abundant Cu_2FeSnS_4 thin films as an efficient counter electrode in dye-sensitized solar cells. *ACS Applied Materials & Interfaces*, 6(20), 17661-17667. doi:10.1021/am503888v

Rudisch, K., Espinosa-García, W. F., Osorio-Guillén, J. M., Araujo, C. M., Platzer-Björkman, C., & Scragg, J. J. (2019). Structural and Electronic Properties of Cu_2MnSnS_4 from Experiment and First-Principles Calculations. *Physica Status Solidi (b)*, 256(7), 1800743. doi:10.1002/pssb.201800743

Shaikh, J., Pawar, R. C., Devan, R. S., Ma, Y.-R., Salvi, P. P., Kolekar, S. S., & Patil, P. S. (2011). Synthesis and characterization of Ru doped CuO thin films for supercapacitor based on Bronsted acidic ionic liquid. *Electrochimica Acta*, 56(5), 2127-2134. doi:10.1016/j.electacta.2010.11.046

Tanaka, T., Kawasaki, D., Nishio, M., Guo, Q., & Ogawa, H. (2006). Fabrication of Cu2ZnSnS4 thin films by co-evaporation. *Physica Status Solidi C*, 3(8), 2844-2847. doi:10.1002/pssc.200669631

Tauc, J. (2012). *Amorphous and liquid semiconductors*. Newyork, USA: Springer. doi:10.1007/978-1-4615-8705-7

Tiong, V. T., Zhang, Y., Bell, J., & Wang, H. (2014). Phase-selective hydrothermal synthesis of Cu_2ZnSnS_4 nanocrystals: The effect of the sulphur precursor. *Cryst Eng Comm*, 16(20), 4306-4313. doi:10.1039/C3CE42606H

Urbach, F. (1953). The long-wavelength edge of photographic sensitivity and of the electronic absorption of solids. *Physical Review*, 92(5), 1324. doi:10.1103/PhysRev.92.1324

Vanalakar, S. A., Patil, P. S., & Kim, J. H. (2018). Recent advances in synthesis of Cu_2FeSnS_4 materials for solar cell applications: A review. *Solar Energy Materials and Solar Cells*, 182, 204-219. doi:10.1016/j.solmat.2018.03.021

Wang, W., Shen, H., Yao, H., & Li, J. (2014). Preparation and properties of Cu_2FeSnS_4 nanocrystals by ultrasound-assisted microwave irradiation. *Materials Letters*, 125, 183-186. doi:10.1016/j.matlet.2014.03.166

Wang, S., Ma, R., Wang, C., Li, S., & Wang, H. (2017). Fabrication and photoelectric properties of Cu_2FeSnS_4 (CFTS) and Cu₂FeSn(S, Se)₄ (CFTSSe) thin films. *Applied Surface Science*, 422, 39-45. doi:10.1016/j.apsusc.2017.05.244

Zhou, J., Yu, S., Guo, X., Wu, L., & Li, H. (2019). Preparation and characterization of Cu_2FeSnS_4 thin films for solar cells via a co-electrodeposition method. *Current Applied Physics*, 19(2), 67-71. doi:10.1016/j.cap.2018.10.014